

## SURFACE MELTING AND THERMAL ABLATION PATTERNS INDUCED IN ENAMEL AND CEMENTUM BY 10.6- $\mu\text{m}$ TEA-CO<sub>2</sub> LASER RADIATION. I. SEM AND AFM ULTRASTRUCTURAL ANALYSIS AND POTENTIAL FOR HARD DENTAL TISSUE PROCEDURES

E. A. PREOTEASA<sup>a\*</sup>, E. S. PREOTEASA<sup>b</sup>, ION N. MIHAILESCU<sup>c</sup>,  
P. LUCUTA<sup>d</sup>, A. MOLDOVAN<sup>c</sup>

<sup>a</sup>*Horia Hulubei National Institute of Physics and Nuclear Engineering (NIPNE), Department of Life and Environment Physics, P.O. Box MG-6, 077125 Bucharest-Magurele, Romania*

<sup>b</sup>*Helident Ltd. Dental Surgery, Bucharest, Romania*

<sup>c</sup>*National Institute for the Physics of Lasers, Plasma and Radiation, P.O. Box MG-, 077125 Bucharest-Magurele, Romania*

<sup>d</sup>*Aerospatial Research Institute, Bucharest, Romania*

*In vitro* studies have demonstrated the potential of CO<sub>2</sub> lasers for various dental enamel treatments with minimal pulpal heating and comparatively low peripheral thermal damage due to short pulse duration. In this study we used a high power TEA-CO<sub>2</sub> laser with pulse length of ~2  $\mu\text{s}$  and very low repetition rate. The ultrastructural effects at nominal fluences of 75, 175 and 625 J/cm<sup>2</sup> on enamel with perpendicular and parallel prisms were examined by scanning electron microscopy (SEM) and atomic force microscopy (AFM). The enamel surface structure of the laser spot boundary and the laser effects on cementum were also studied. At 75 J/cm<sup>2</sup> a rather uniform glazing of enamel adequate for caries prevention was produced. The fluence of 175 J/cm<sup>2</sup> created a rough surface by exfoliating the prism crystals. At 625 J/cm<sup>2</sup> the laser pulses with Gaussian profile produced bubbles in the center of the spot. Most remarkably, they were surrounded by concentric wave-like patterns, not reported in previous studies on enamel, although similar periodic structures were produced before with shorter laser pulses on the surface of inorganic materials. The wave structure and periods were strongly dependent on the enamel prisms orientations, suggesting energy absorption dependence on the surface defects density. In the irradiated enamel with perpendicular prisms, the AFM-measured roughness vs. fluence showed a threshold and an asymptotic saturation. The ultrastructure of the spot boundary was also different according to the prisms orientation. Outside the spot calcination of enamel was observed. In cementum, a moderate surface melting was produced at 75 J/cm<sup>2</sup>, while at 625 J/cm<sup>2</sup> explosive hydrokinetic ablation occurred due to residual water in the pores. For dental applications one could make use of the enamel surface roughening associated to the periodic patterns and the bubbles produced at 625 J/cm<sup>2</sup>, and to the flaked-off surface generated at 175 J/cm<sup>2</sup>. This could improve the bond strengths of composites adhesion to enamel in drill prepared cavities and on sealed molar grooves. Treatments of periodontitis should use low fluences (~75 J/cm<sup>2</sup>) to prevent hydrokinetic ablation of cementum. To control the dependence of the ablation patterns produced in enamel at 625 J/cm<sup>2</sup> on the orientation of prisms, prior structural diagnosis should be necessary. Special optical diagnosis devices should be engineered for this purpose.

(Received May 5, 2013; Accepted July 22, 2013)

**Keywords:** TEA-CO<sub>2</sub> laser, SEM, AFM, Dental enamel, Prism orientation, Ablation pattern, Periodic structures, Boundary effects, Dental cementum, Dental procedures potential

---

\* Corresponding author: eugenpreoteasa@gmail.com.

## 1. Introduction

Laser applications in dentistry are extremely diverse, leading to valuable clinical results both on hard and soft tissues [ 1 – 3]. Many clinical applications based on thermal effects and using powerful IR<sup>†</sup> lasers with Nd:YAG, Nd:YAP, Ho:YAG, Er:YAG, Er,Cr:YSGG and CO<sub>2</sub> as active media have been reviewed [4, 5]. In this area, the CO<sub>2</sub> laser enjoys a respectable position not only for historical reasons [6] but also for its practical performances. The undisputed field of the CO<sub>2</sub> laser is in the oral and maxillofacial surgery [7] and periodontics [8] due to its excellent control of soft oral tissues hemorrhage and bleeding. Other applications include implantology [9], treatment of peri-implantitis [10], sterilization of pulp, dentin, periapical and other dental infections [11, 12], treatment of vertical root fracture [13, 14], guided tissue regeneration, prosthetics [7, 10 ], orthodontics and debonding of orthodontic brackets [15 ], and activation of teeth bleaching agents [13].

The dental applications of the CO<sub>2</sub> laser thermal effects are based on the strong absorption of its radiation by water from soft tissues and by hydroxyapatite from enamel, dentin and cementum. At present, the US Food and Drug Administration did not yet approve the use of the CO<sub>2</sub> laser on hard tissues [7] except for tooth whitening [16]. But from the above it is obvious that some applications are being extended beyond the soft tissues. The laser radiation interactions with the teeth and/or with dental materials still offer great potential in dentistry – and research in this direction is being continued [17, 18].

The irradiation of hard tissues with the CO<sub>2</sub> laser aims the treatment of caries which involves cavity preparation by thermal [19, 20] and hydrokinetic [21] ablation, the surgery of maxilo-facial bones [22], and the caries prevention by surface modifications of enamel and dentin which reduce their demineralization [17, 23 – 25]. In the most straightforward approach protection against caries lesion onset and development is done by crystal melting and fusion of surface enamel layer for a sealing effect at relatively low laser fluence. The use of pulsed CO<sub>2</sub> lasers for this type of applications is favoured by confined thermal changes in a layer not deeper than 40 μm [14, 26] and a neglectible heating at the level of the pulp [27 – 29]. In related studies, the CO<sub>2</sub> laser irradiation of dentin improved the occlusion of the dentinal tubule orifices by a bioglass mixed with phosphoric acid [30] and increased the shear strengths of glass-infiltrated alumina ceramics bonded to dentin [31]. CO<sub>2</sub> laser irradiation combined with fluoride inhibited the demineralization of cementum on the root surface [32] and of enamel [33, 34]. The prevention of enamel demineralization was obtained also by CO<sub>2</sub> laser fusion of synthetic hydroxyapatite as a sealant for pits and fissures [35]. However, research is still needed in order to reduce detrimental effects of CO<sub>2</sub> lasers such as cracking, fissuring and disruption of enamel rods, carbonisation of dentinal tubule contents, excessive loss of tooth structure [36] and loss of the odontoblastic layer [14].

In addition to forming the object of a large volume of clinically-directed research, the complex interactions of the CO<sub>2</sub> laser radiation with the hard tissues were also studied from a physical perspective (both experimental and theoretical) [21, 37 – 42]. To account realistically for the properties of the biological tissues, some theoretical models proposed for various types of lasers describe tissues as heterogeneous [43] and anisotropic [44] media. In fact the enamel has an inhomogeneous and anisotropic structure. PIXE elemental analysis evidenced differences between cusps of the same tooth [45]. SEM studies have found cusp dissimilarities in the enamel prism areas, density and packing [46].

Refractive index and absorption coefficient of dental enamel at CO<sub>2</sub> laser wavelengths highlighted a directional dependence of the optical constants, which may be important for surface

### <sup>†</sup> Abbreviations and acronyms:

AFM – atomic force microscopy; CW – continuous wave; FEL – free electron laser; FT – Fourier transform; FTIR spectrometry – Fourier transform infrared spectrometry; HA – hydroxyapatite; IR – infrared; OM – optical microscopy; PIXE – particle-induced X-ray emission; RMS – root mean square; SEM – scanning electron microscopy; TEA – transversely excited, atmospheric pressure; YAG – yttrium-aluminium-garnet (Y<sub>3</sub>Al<sub>5</sub>O<sub>12</sub>); YAP – yttrium-aluminium-perovskite; YSGG - yttrium-scandium-gallium garnet; XPS – X-ray photoelectron spectroscopy.

treatment of teeth and fusion of dental materials [47]. Differences in the ultrastructure of irradiated dentin were observed depending on CO<sub>2</sub> laser irradiation direction, i.e. parallel and perpendicular to the root canal walls [48]. CO<sub>2</sub> laser-induced surface alteration like flaked off material depends on the parallel and perpendicular prism orientation [49, 50]. These few studies suggest that more investigation is needed for a better understanding of this interesting directional effect.

The transversely excited atmospheric pressure (TEA) CO<sub>2</sub> laser at 10.6 μm could be suitable for such studies, because due to its high power and short pulses it is highly appreciated since the '90s for ablating dental hard tissue [13]. Moreover, in search for a precise ablation of hard tissues without significant thermal side effects, the CO<sub>2</sub> TEA laser (0.1 – 2 μs pulse length) could fill a gap between the pioneering studies [6] who used a simple CO<sub>2</sub> laser with pulses 50 μs long and the developments using a highly sophisticated Nd:YLF laser system with picosecond or femtosecond pulse durations; the later produced plasma-induced ablation without significant thermal and mechanical damage [41]. By comparison, it is obvious that the robust TEA-CO<sub>2</sub> laser is a cost-effective solution. Another reason for the choice of the thermomechanical ablation by TEA-CO<sub>2</sub> laser is that the microexplosions occurring in the hydrokinetic ablation, a method very popular these days, may induce cracks up to 300 μm deep that can be the origin for new caries development [41, 51, 52].

The previously discovered bond strength increase of ceramics glass ionomers to dentin by CO<sub>2</sub> laser irradiation [31] raises the question whether a similar improvement of restorative materials bonding could be obtained for enamel after laser modification of its surface structure. To this purpose the roughness of the enamel surface on the micrometer or nanometer scale should be increased. The roughening of the surface by inducing patterns of frozen waves was described for metal targets (review in [53]), for electroinsulating inorganic crystals [54, 55] and for metallic nitride ceramic multilayered coatings [56] by using CO<sub>2</sub> and other lasers with nanosecond to femtosecond pulses. Therefore the search for such a possible effect in enamel irradiated with the microsecond pulses of the TEA-CO<sub>2</sub> laser would be relevant both basically and for potential applications.

Here we report a study by SEM and AFM on the effects produced by TEA-CO<sub>2</sub> laser irradiation on teeth having different orientations of enamel prisms. As compared to other surface topography analysis methods like μ-PIXE [45], μ-FTIR [57] and μ-Raman spectroscopy [58], these microscopy techniques have a better resolution and some other definite advantages. For instance SEM images allow a wide range of magnifications and have an enhanced contrast and a large depth of field, yielding a characteristic three-dimensional appearance of the surface structure, while AFM allows the measurement of surface roughness. In addition to the ultrastructure of the spot, its boundary is studied because the laser irradiation usually does not cover the whole surface of a tooth. The effects of cementum and cementoenamel junction irradiation are studied for the interest of the TEA-CO<sub>2</sub> treatments of periodontal diseases. The potential of the results for hard dental tissue procedures of clinical interest is discussed. In the second part of this study, simple physical models are proposed for the interpretation and a better insight of the laser-induced changes in the surface ultrastructure.

## 2. Materials and methods

### *Dental samples*

Permanent teeth from adult patients were extracted in order to solve periodontal and therapeutic dental problems. Three teeth presenting relatively large and approximately flat areas of sound and scale-free enamel were selected for laser irradiation. As seen with an optical microscope in reflected light, they were an upper central incisor (Fig. 1A), a lower molar (Fig. 1B) and an upper wisdom tooth (Fig. 1C). The teeth were washed with tap and distilled water after extraction and kept provisionally in a saturated humid environment in sealed plastic bags. To simplify the experiment, the organic traces from their surface enamel layer were removed by incubation in hydrogen peroxide 10% for about 1 month. The excess humidity was then removed by keeping the

teeth in dry air at room temperature for several days before use. The preparation ensured a clean surface.

The irradiated enamel spots of 5 mm diameter are shown marked with circles on the teeth in Fig. 1A – 1C. The surface microstructures of the native, non-irradiated enamel from areas adjacent to the spots as observed by SEM are shown in Fig. 1D, 1E and 1F, respectively, below the corresponding tooth.

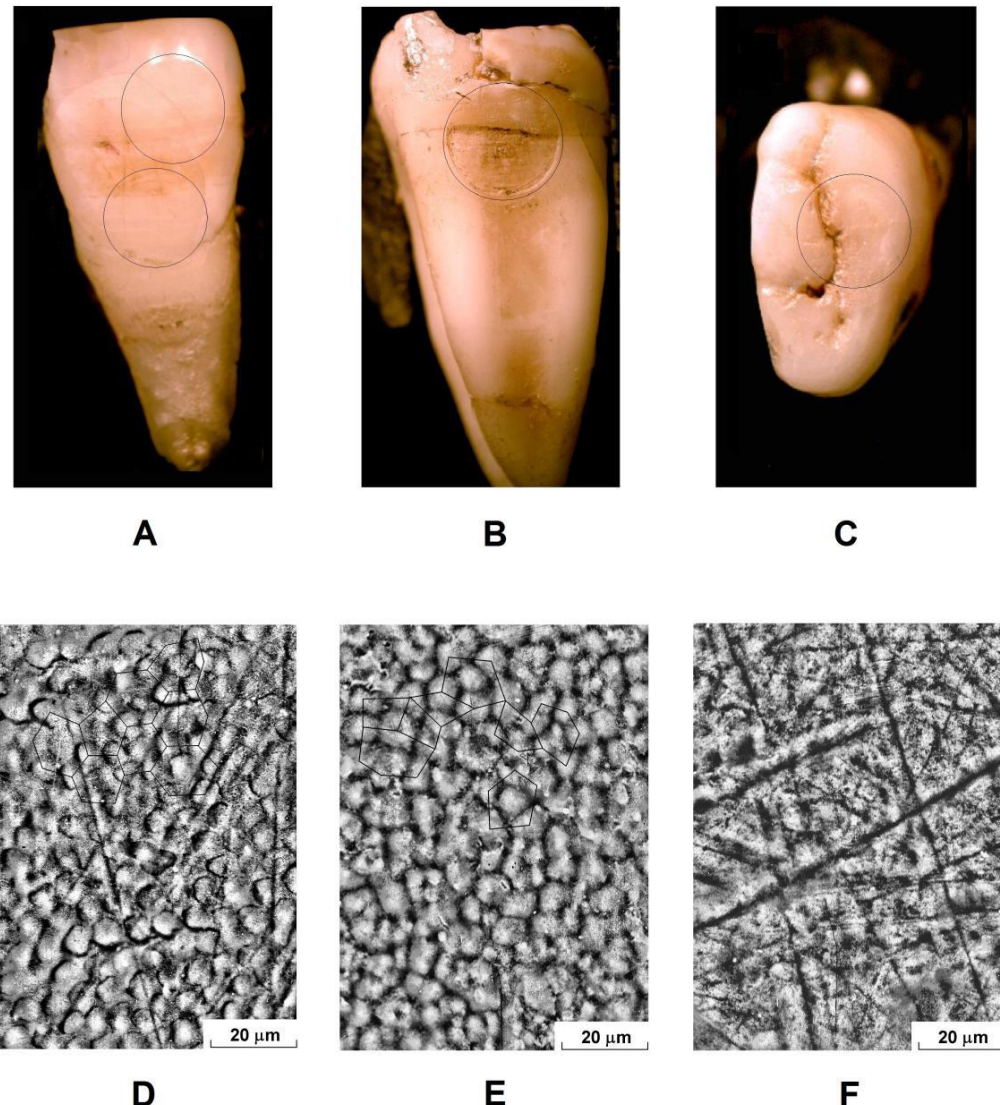


*Fig. 1. The laser irradiated teeth images by reflectance OM (top) and the SEM ultrastructure of their native enamel surfaces in areas adjacent to spots (bottom). A, D – upper incisor; B, E – lower molar; C, F – wisdom tooth. The laser spots are shown by circles in images A, B, C. The enamel prisms are perpendicular on the surface in images D and E, and parallel in image F. The organization of perpendicular prisms outlined in images D and E by thin lines connecting the centers of prisms was more regular in the upper incisor than in the lower molar.*

#### *The surface structure of native enamel*

Basically, the unirradiated enamel as seen by SEM may have the crystalline prisms perpendicular as in the upper central incisor (Fig. 1D) and in the lower molar (Fig. 1E) or parallel to the surface as in the wisdom tooth (Fig. 1F). The shape of the prisms' heads in the incisor enamel was quasi-circular while in the lower molar it was irregular. The mean distances of about 7  $\mu\text{m}$  between the centres of prisms including their diameter and the interprismatic spaces filled with less ordered hydroxyapatite crystals (Table 1), were negligibly smaller in the incisor than in the lower molar, but the corresponding standard deviation was about twice larger in the later case due to the prism shape variability.

*Table 1. The teeth characteristics and the irradiation conditions of the dental specimens with the pulsed CO<sub>2</sub> TEA laser radiation of 10.6  $\mu\text{m}$*

Tooth	Orientation of enamel prisms relative to surface <sup>1</sup>	Enamel prism size $\mu\text{m}$	Enamel prism density $\mu\text{m}^{-2}$	Enamel surface defects density		Irradiated area of tooth	Number of laser pulses <sup>2</sup>	Nominal fluence, <sup>3-5</sup> J/cm <sup>2</sup>
				Point-centred, $\mu\text{m}^{-2}$	Fili-form, $\mu\text{m}^{-1}$			
Upper central incisor	Perpendicular	7.0 $\pm$ 0.6	(2.1 $\pm$ 0.4) 10 <sup>-2</sup>	$\sim$ 7 10 <sup>-1</sup>	Vestibular face, at a secant level of CEJ	3	75 $\pm$ 16	
					Vestibular face, near the incisor edge	7		175 $\pm$ 25
Lower molar	Perpendicular	7.1 $\pm$ 1.1	(2.1 $\pm$ 0.7) 10 <sup>-2</sup>	$\sim$ 4 10 <sup>-1</sup>	Mesial face, at a diametrical level of CEJ	25	625 $\pm$ 46	
Upper wisdom tooth	Parallel	n.d.	n.d.	$\sim$ 5 10 <sup>-6</sup>	$\sim$ 10 <sup>-2</sup>	Occlusal face	25	

<sup>1</sup>As observed by SEM of native (unirradiated) enamel adjacent to the spots, Fig. 1.

<sup>2</sup>Energy per pulse (output from the laser, uncorrected):  $\sim$ 5 J with the instrumental conditions as described. The values of energy directed to the spots were of  $\sim$ 15,  $\sim$ 35,  $\sim$ 75 and  $\sim$ 75 J, respectively.

<sup>3</sup>Spot diameter 4.9  $\pm$  0.1 mm, spot surface  $\sim$ 0.2 cm<sup>2</sup>. Nominal fluence of laser radiation output is given. It is assumed to be equal with the fluence incident on samples, estimated without corrections for losses in the AR germanium lens and air.

<sup>4</sup>An estimate of the effective fluence due to absorbed radiation energy, accounting for the losses due to plasma formation (50 - 70%), to reflection and to scattering ( $\sim$ 5% and  $\sim$ 10% of the remaining, respectively [59]) – but not for the differences due to enamel prisms orientation – gives roughly 25  $\pm$  12 J/cm<sup>2</sup> (3 pulses), 60  $\pm$  28 J/cm<sup>2</sup> (7 pulses) and 212  $\pm$  100 J/cm<sup>2</sup> (25 pulses); the errors are intentionally overestimated.

<sup>5</sup>The errors of the nominal fluence were estimated with the formula  $\varepsilon = \varepsilon_0 N^{1/2}$  assuming independent action of the successive pulses and applying the error propagation formula (cf. [60]). Here  $\varepsilon_0$  is the error in the evaluation of fluence delivered by a single pulse and  $N$  is the number of applied pulses. However the errors should be somewhat higher if taking into account the errors associated to reflection and scattering strongly dependent of prisms orientation, as well as those associated to the reproducibility of the laser output energy per pulse.

Accordingly, the  $2\sigma$  confidence limits of the prism size were between  $5.8 - 8.1 \mu\text{m}$  in the incisor as compared to a broader range of  $5.0 - 9.2 \mu\text{m}$  in the lower molar. The packing structure and symmetry of the prisms is different in the upper incisor and lower molar enamel. In the upper incisor they are disposed in distorted centred hexagons and rarely pentagons, like in a quasi-crystalline 2D geometry (Fig. 1D). In the lower molar, they form an amorphous arrangement, without any obvious long distance order, although their 2D distribution displays locally distorted hexagons and pentagons and irregular quadrangles (Fig. 1E).

The linear density of prisms in the incisor is somewhat larger along the  $x$  direction of Fig. 1D as compared to the  $y$  direction, while the lower molar appeared two-dimensionally isotropic (Fig. 1E). The packing in terms of interprismatic spaces between prisms is more dense in the molar than in the incisor enamel, although their mean surface density is the same ( $\sim 2 \cdot 10^{-2} \mu\text{m}^{-2}$ ) within errors. This means that at variance to the lower molar, the incisor contained more interprism enamel with the hydroxyapatite crystallites oriented differently (e.g., at  $\sim 45^\circ$ ). In the case of the upper wisdom tooth with parallel prisms (Fig. 1F) such a detailed ultrastructural characterization is not possible because the prism heads are not visible.

The enamel surface showed natural or acquired morphological defects (small cavities or pores, prominences and striations) which are primary sites of attack in the early demineralization stages leading to caries formation. On the surface of enamel with parallel prisms of the wisdom tooth one can see point-centered formations somewhat like flowers and low mounds, as well as many linear scrapes (Fig. 1F) and zigzag or branched fissures (upper inset of Fig. 5E). The enamel with perpendicular prisms of the incisor shows also scrapes (Fig. 1D) and fissures (inset of Fig. 5A). But most important the interprismatic junctions provide a surface network of filamentary or quasi-unidimensional defects, and the prisms' heads may be looked at like point-centered defects (Fig. 1D, 1E, 3A inset, and 5A). We evaluated a much higher surface density of defects on the upper incisor and lower molar enamel with perpendicular prisms, as compared to the wisdom tooth with parallel prisms (Table 1). The point-centred defects amounted to  $\sim 2 \cdot 10^{-2} \mu\text{m}^{-2}$  in the first case and to only  $\sim 5 \cdot 10^{-6} \mu\text{m}^{-2}$  in the second. The corresponding figures for quasi-one-dimensional, filiform defects were of close orders of magnitude ( $\sim 4 - 7 \cdot 10^{-1} \mu\text{m}^{-1}$  and of  $\sim 10^{-2} \mu\text{m}^{-1}$ , respectively). Although this evaluation was very approximative, it evidenced orders of magnitude differences of surface point-like defect density between the studied areas around the laser-irradiated spots on the incisor and lower molar on one side and the wisdom tooth on the other.

The results showed that these ultrastructural parameters could play important roles in the laser-induced surface alteration effects.

### *Laser irradiation*

A pulsed CO<sub>2</sub> laser excited by transversal electric discharges at atmospheric pressure (TEA) with preionization [61] of the Lamberton-Pearson type [62, 63] was used. The laser had helically arranged electrodes and was assembled by three discharge tubes to ensure a larger active volume and thus higher energy per pulse. It was operated at 40 kV in a CO<sub>2</sub>-N<sub>2</sub>-He gas mixture (5:5:90 v/v) doped with xylene vapours and generated 10.6  $\mu\text{m}$  wavelength radiation [64 – 67]. The beam had an approximately Gaussian profile. The laser pulse energy was measured with a Hadron 120 B energy meter, and a time display of the pulse was recorded with a germanium photon drag detector. With the described setup, radiation pulses of  $\sim 5 \text{ J}$  energy with a shape typical for TEA-CO<sub>2</sub> lasers: a sharp peak with a halfwidth of  $\sim 150 \text{ ns}$  and a tail which lasts 2 – 10  $\mu\text{sec}$  duration, were obtained at 10 – 12 sec time interval in a pulse-by-pulse controlled regime. The beam was focused in a spot of about 5 mm diameter with an antireflex (AR) coated germanium lens of 5.1 cm focal distance with antireflection coating. The irradiated tooth samples' surface was vertical and perpendicular to the beam and the distance to the lens was preselected with test specimens.

In the design of the teeth irradiation (Table 1) we adapted the general concept of a screening by a few fluence values in approximately geometric progression covering a large range [6, 23]. However our conditions (5 J per pulse,  $\sim 2 \mu\text{s}$  pulse duration,  $0.15 - 0.20 \text{ s}^{-1}$  repetition rate)

were completely different, i.e. shorter pulse length, higher energy per pulse and lower repetition rate. A detailed discussion is needed to explain the rationale for the irradiation conditions.

A definite advantage expected for the shorter pulses delivered by the TEA-CO<sub>2</sub> laser could be the ability to produce precise ablation of hard dental tissues without major thermal damage (e.g. cracks, fissures) by reducing heat diffusion in the time frame of pulse duration [41, 68]. Implicitly the pulsed CO<sub>2</sub> lasers provide protection of the pulp against heating (e.g. from < 1°C at 2 mm depth with a fluence of 12.5 J/cm<sup>2</sup> per pulse [24] to ~3 °C with an incident fluence of 20 J/cm<sup>2</sup> [28]). Moreover due to the low repetition rate used the effects of successive pulses were thermally isolated of each other as the enamel could return close to room temperature during the long time between pulses (10 – 12 s). Thus the morphological effects cumulated more or less additively without major cooperative build-up of thermomechanical effects.

In our experiment, the upper incisor was irradiated on two distinct spots with 3 and 7 pulses, respectively, while the lower molar and the upper wisdom tooth received 25 pulses per pulse. Thus the resulting nominal fluence (emitted from the laser) focused in spots of 5 mm diameter was almost one order of magnitude higher as compared to the cited studies [6; 23]. However the term ‘fluence’ is used in various senses in dental studies and there is some uncertainty and approximation in the literature fluence values. One has to distinguish between the ‘nominal’, emitted and measured [69, 70], incident [28] or applied, and absorbed [23] or ‘effective’ fluence. The latter accounts for the appreciable loss in the effective energy density due to plasma formation, which could not be evaluated precisely (except by specially designed measurements) and which is particularly important for the TEA-CO<sub>2</sub> laser.

The nominal fluence we used per single pulse was 25 J/cm<sup>2</sup> and was selected by reference to the threshold values for effects produced by pulsed 10.6 μm radiation on enamel. Thus chemical modifications were detected by FT-Raman spectroscopy at 6.0 J/cm<sup>2</sup> and also ultrastructural changes as seen by SEM were reported [69]. Still, other authors did not detect by SEM surface melting and crystal fusion below 20 J/cm<sup>2</sup> [23]. Inhibition of caries-like lesions produced by *in vitro* demineralization was evidenced by microradiography starting from 13 J/cm<sup>2</sup> [6] and from 25 J/cm<sup>2</sup> by cross-sectional microhardness testing [24]. Also, at 25 J/cm<sup>2</sup> the first macroscopic effects (surface opacity) could be produced on enamel with a sequence of longer and less energetic pulses [6]. Hence there is some unconformity in the threshold values depending on the applied laser pulse sequences and on the methods used for assessing the changes. However at a nominal fluence of 25 J/cm<sup>2</sup> per pulse, we could expect that each single pulse produced ultrastructural changes observable by SEM and AFM and, moreover, potentially relevant for the protection of enamel against caries progression.

The lowest nominal fluence of 75 J/cm<sup>2</sup> produced by 3 pulses was selected to make sure not only for the generation of ultrastructural changes observable by SEM and AFM, but also for some minimal macroscopic changes of the enamel surface visible with a reflexion optical microscope. Even so, the spot irradiated with 3 pulses was extremely faint and hard to see (Fig. 1A lower spot). This approach facilitated the observation of the spot’s margin, which is of potential dental interest for treatments not covering the whole tooth surface. Although it exceeds the threshold for gross surface alterations, the above fluence is typical for the caries prevention in dental enamel and remains close enough to the threshold of caries inhibition so as to expect less important disruptive effects due to shock wave generation [41].

The middle nominal fluence of 175 J/cm<sup>2</sup> corresponding to 7 pulses laid near the limit between the caries prevention domain of fluencies and the laser ablation domain for caries treatment and cavity preparation. For instance with 9.3 μm pulses and a lower fluence – which could be considered roughly equivalent to our fluence of 7 pulses at 10.6 μm as suggested by comparative studies [23] – craters were drilled in enamel [70].

The highest nominal fluence of 625 J/cm<sup>2</sup> applied with 25 pulses delivered on the lower molar and the upper wisdom tooth should be typical for CO<sub>2</sub> laser ablation of enamel. Nevertheless, irradiation with 0.3 J/cm<sup>2</sup> per pulse of 5 μs at 226 Hz and cumulating a total fluence of about 610 J/cm<sup>2</sup> was performed in order to increase caries resistance [68, 71].

The corresponding ‘effective’ fluences for the 3, 7 and 25 applied pulses were evaluated to 25, 60 and 212 J/cm<sup>2</sup> (footnote 4 of Table 1), but they are only a rough guide because we found the interaction of the laser beam with the enamel to depend critically on the orientation of the enamel

prisms. These values are more close to the caries prevention fluence range. However a clear-cut boundary between the fluence ranges appropriate for caries inhibition and caries removal seems to be not possible, both because the two domains seem to overlap and because the threshold values are approximate, depending on the laser pulse and sequence parameters as well as on the definition of fluence. In brief, the enamel irradiation with 3, 7 and 25 pulses covered a range of fluences with effects extending potentially from caries prevention to caries treatment by enamel ablation.

#### *Scanning electron microscopy*

The surface morphology of control and laser-irradiated enamel was examined by SEM in secondary electron imaging regime with a JXA-50 Electron Probe Microanalyzer (Jeol, Tokyo, Japan), an instrument which allows a resolution of 10 nm or better. The electroinsulating surface of teeth was coated with a thin (20-40 nm) film of carbon by vacuum evaporation at  $10^{-5}$  torr to prevent charging and associated image artifacts and to enhance the yield of secondary electrons.

Areas of native and laser-irradiated enamel as well as of the boundary zones between the two contiguous regions were selected with the adjustable sample stage. By appropriate choice of working distance and acceleration voltage, nominal magnifications of  $\times 50$  to  $\times 2500$  were used. The scale of the SEM images at  $\times 1000$  and  $\times 2000$  magnifications is similar to that of the AFM images.

#### *Atomic force microscopy*

AFM images were taken with an XE-100 instrument (Park Systems, S. Korea) operated in the noncontact mode, using a silicon tip of 10 – 20 nm radius. A scanning rate of 0.2–0.3 lines  $s^{-1}$  was used, as a function of topography and scanned area. The laser irradiated spots were observed and nearby zones of unirradiated enamel were used as controls. Three or two distinct square fields of 20  $\mu m$  sides were scanned on each examined area. Root mean square (RMS) roughness measurements of the areas were performed using the incorporated XEI soft. Control optical microscopy images of the sample were taken with the incorporated microscope at a magnification of  $\times 300$  –  $\times 780$ .

### **3. Results and discussion**

#### *Enamel ablation at low and intermediate fluence*

On the incisor surface observed with the optical microscope in reflected light (Fig. 1 A), the spot partly overlapping the cementoenamel junction which was irradiated with 3 pulses summing up  $75 \text{ J/cm}^2$  nominal fluence was hardly visible and only in grazing light. It looked like a patch somewhat bleached and slightly more opaque than the surrounding enamel. The irradiation with 7 pulses ( $175 \text{ J/cm}^2$  nominal fluence) of the spot near the tooth edge produced a little more pregnant discoloration and an extremely slight depression on the enamel surface, probably associated with an incipient ablation. The two circular spots of about 5 mm diameter presented in common a macroscopic aspect a bit more unpolished than the outside enamel around.

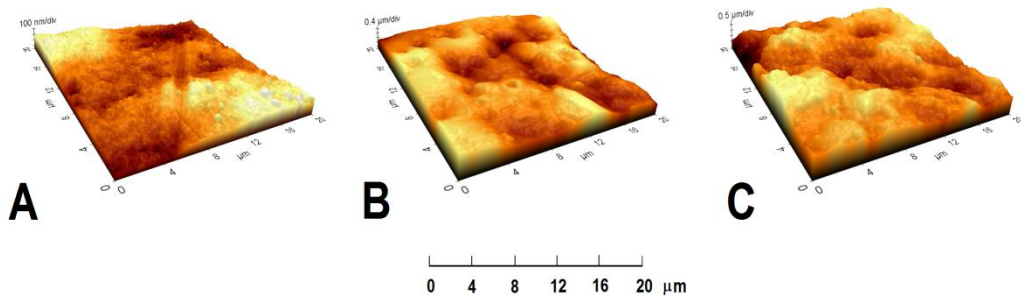


*Fig. 2. – AFM maps of upper incisor enamel with perpendicular prisms irradiated at low and intermediate fluence. A, native; B, irradiated at 75 J/cm<sup>2</sup> fluence; C, irradiated at 175 J/cm<sup>2</sup> fluence.*

The AFM maps of unirradiated, native enamel evidenced many small peaked irregularities of 100-200 nm height and of 0.5-1 μm diameter (Fig. 2A). After the 75 J/cm<sup>2</sup> irradiation (Fig. 2B), these small relief forms were no longer observed. The surface looked rather smooth, amorphous and glassy with valleys and hills up to ~1 μm high and about 5 μm in size. At 175 J/cm<sup>2</sup> nominal fluence (Fig. 2C) these large forms become higher up to ~2 μm and the aspect of their surface was less smooth and glassy, being covered with small irregularities of about 0.5 μm size. Both irradiated spots evidenced thus clearly the superficial melting of enamel, but with particularities depending on the fluence.

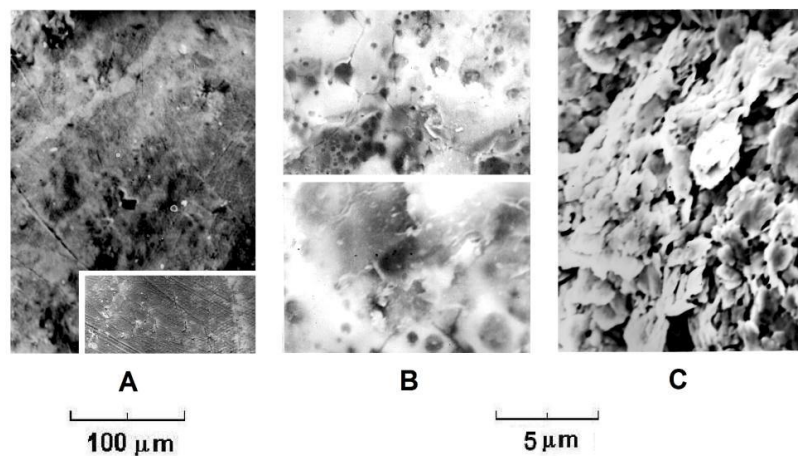


*Fig. 3. SEM images of native (A) and laser-irradiated enamel of the upper incisor with perpendicular prisms exposed to low and intermediate fluence of 75 J/cm<sup>2</sup> (B) and 175 J/cm<sup>2</sup> (C).*

The SEM images of the incisor produce further insight. While the unirradiated zones show at a higher magnification the enamel prisms perpendicular on the surface with appreciable interprism enamel (Fig. 1D), at a lower magnification the prisms still can be seen (Fig. 3A inset) and various defects such as small but rare cavities are observed (Fig. 3A).

At a magnification comparable to the AFM images, the spot irradiated with 75 J/cm<sup>2</sup> (Fig. 3B) shows a smooth and glassy surface with larger protuberances of about 5 μm diameter and with numerous small (0.5-1 μm) cavities and rare larger (up to 2 μm) hollow spaces. Moreover the glazed enamel showed narrow fissures probably due to tensions appeared during cooling which were not seen in the AFM pictures.

The aspect of the enamel irradiated at 175 J/cm<sup>2</sup> (Fig. 3C) was no longer smooth and glassy and revealed a conglomerate, flaked-off structure resulted by some kind of exfoliation and

not evidenced by AFM. The surface appears to be rough and decorated with stacked elements of 2–3 µm, looking like flakes or tree bark. This unusual structure seems to be a loose formation made up by ablation scraps protruding from the ablated surface. Flaked-off products material has been produced by pulsed laser ablation of materials so diverse as polyimide film [72] and dental enamel with parallel prism orientation [50]. Also the CO<sub>2</sub> laser showed a tendency to detach material in the head of the enamel prisms where crystallites ran parallel to the long axis of the prism [49]. therefore The observed flakes from Fig. 3C may be detached hydroxyapatite crystals either from the perpendicular prisms or from the interrod enamel where the crystals are oriented in a different direction (whichever is more favourably oriented). Alternately, the exfoliation of a quasi-homogeneous polymer film [72] suggests that the flakes could be small drops of melted enamel which were spread radially by rampant boiling during the laser beam impact. They probably began to solidify before reaching the solid enamel surface and adhered to it in a semi-solid state aggregating themselves in a layer stacked on the surface.

Note that the effects of the CO<sub>2</sub> laser irradiation at low and intermediate fluence – which explain the increase in enamel's acid resistance – are very complex and include, in addition to the decrease of the enamel permeability by fusion of the enamel surface ultrastructure, other alterations such as inhibition of the ion diffusion into enamel by decomposition of the protein matrix, and reduction of solubility by recrystallization and chemical changes (reduction of water and carbonate contents, altered calcium–phosphate ratio, increase in hydroxyl ion contents, formation of pyrophosphates, etc.) [73].

#### *Patterns of enamel thermal ablation at high fluence*

Changes like carbonate loss, crystallographic restructuring, and fusion of enamel could be even more important in the high fluence domain, but among them we examined only the results of melting and resolidification of enamel as seen in the changes of surface micro- and ultrastructure. In enamel, the typical macroscopic effect of laser irradiation with 25 pulses – yielding a nominal fluence of  $625 \pm 46 \text{ J/cm}^2$  (and estimated effective fluence of  $212 \pm 100 \text{ J/cm}^2$ ) – was the formation of rather shallow depressions (Fig. 1B and 1C). On the other hand an appreciably deeper crater was produced in the cementum of the lower molar (Fig. 1B). The SEM examination of the shallow craters produced by 25 laser pulses in the enamel of both teeth evidenced disordered structures in the central areas of the spots and clear periodic patterns at the periphery (Fig. 4A and 4B). To our knowledge, this is the first report of periodic patterns produced by CO<sub>2</sub> laser irradiation of dental enamel. The particular characteristics of the altered surface morphology patterns were different on the two samples according to the orientation of the enamel prisms with respect to the natural surface of the teeth (Fig. 4A and 4B). The structural differences seen in the irradiated enamel correlate with the different orientation of prisms – perpendicular in the lower molar (Fig. 1E) and parallel in the wisdom tooth (Fig. 1F) –, emphasizing the postulate of a strong dependence of the laser effects on the native enamel's ultrastructure.

#### *Quasi-periodic enamel patterns at high fluence*

Both teeth irradiated with 25 pulses showed concentric, radial wave patterns in the peripheric region nearby the margin of the spot, where the radiation intensity of the beam with quasi-Gaussian profile was lower (Fig. 4A, 4B, and 5B, 5F). In the upper panel of Fig. 5 SEM images of the lower molar's mesial face with perpendicular prisms are shown in detail. The lower panel displays the occlusal face of the wisdom tooth with the prisms parallel to the surface. The periods of the waves increased progressively up to the maximum radius of the spots (~2500 µm). The occurrence of these periodic patterns suggests that waves are formed in the surface enamel layer melted by the laser pulse. The solidified waves could be due to thermo-mechanical effects due to fast local dilatation of the melted substance, to modeling of the ablation pattern in the molten enamel by plasma or acoustic waves, or to both of them.

The periodic patterns – regardless of their formation mechanism(s) – were different according to the orientation of the enamel prisms. In the mesial face enamel of the lower molar

with perpendicular prisms they were spaced  $42 \pm 2 \mu\text{m}$  apart (Fig. 4A, 5B); in the occlusal face enamel of the wisdom tooth with parallel prisms their periods were of  $68 \pm 7 \mu\text{m}$  (Fig. 4B, 5F). Also, the increase in the periods of the radial waves near the periphery of the spot is more visible on the enamel with parallel prisms of the wisdom tooth.

Moreover, on the enamel of the lower molar with perpendicular prisms, we observed a superimposed second pattern of waves with shorter period of  $11.0 \pm 1.5 \mu\text{m}$  (lower image of Fig. 5B). These were genuine details and could not be due to parasitic SEM effects because they have been observed in different zones and with different magnifications. However, their wavelength was very close to the  $\lambda = 10.6 \mu\text{m}$  radiation, and one cannot rule out the possibility that these short waves could be produced in enamel by a diffraction pattern of the incident laser beam. The short wavelength periodic patterns were often grouped in trains of about 10 waves. The orientation of their wavefronts was frequently quasi-perpendicular to the radial waves of  $42 \mu\text{m}$  (upper panel of Fig. 5B) and sometimes quasi-parallel (lower zone of Fig. 4A, visible on higher magnification). In other zones they formed complicated motifs with parallel curves (lower panel of Fig. 5B). However in each examined area they were oriented within approximately less than  $\pm 30^\circ$  about a preferential direction. The observed waves of  $\sim 11 \mu\text{m}$  showed many features which are characteristic to the so-called ‘resonance periodic structures’ which were induced by CO<sub>2</sub> laser irradiation at the surface of metal targets [53], first of all their period  $\Lambda$  close to the radiation wavelength  $\lambda$  but also their preferential orientation. They arise by interdependent electrodynamic and thermophysical mechanisms which are not yet fully understood, as their origin is very complex and non-singular (review in [53]). In such models the period  $\Lambda \sim \lambda$  is due to the interference between the incident / scattered / diffracted and/or refracted waves which creates strong lateral temperature gradients along distances of the order of  $\lambda$ . Consequently the corresponding gradients of temperature-dependent properties of the melted material result in spatial waves with periods close to the laser radiation wavelength.

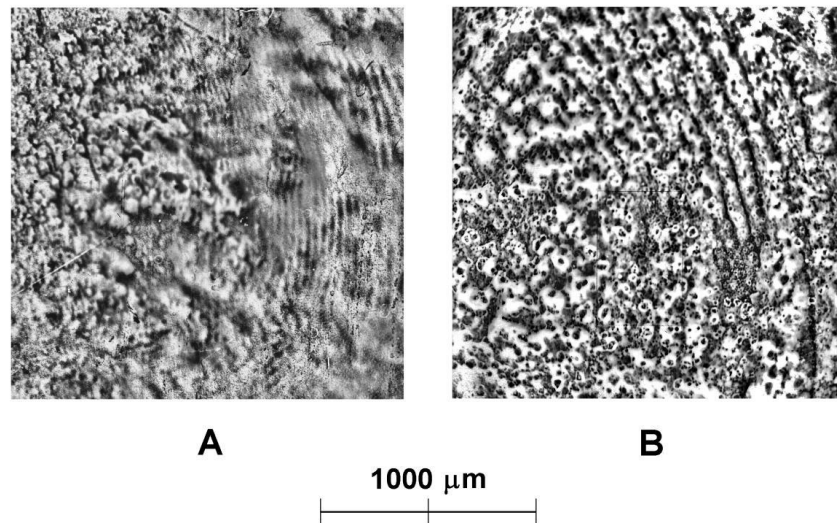


*Fig. 4. – SEM images of high fluence ( $625 \text{ J/cm}^2$ ) ablation patterns in enamel with perpendicular (A) and parallel (B) prisms showing bubbles at the center of the spots and concentric waves in the outer regions.*

Possible explanations of the laser ablation patterns dependence on enamel structure are discussed in Part II of this study. However, one can assume a higher absorption of energy in the enamel with perpendicular prisms due to the higher density of defects on its surface as compared to the one with parallel prisms. In fact the formation of resonant periodic structures is favoured by the presence of defects on the irradiated surface [53], and the resonant periodic structures were observed only on the enamel with perpendicular prisms. The surface defects should play a similar role in the case of the waves with longer periods (42 and  $67 \mu\text{m}$ ). Another factor possibly involved

could be the anisotropy of the enamel surface layer, because one can expect different coefficients of thermal conductivity and dilatation along the longitudinal and transversal prism axes, and the orientations of prisms were different. Therefore, various thermo-mechanical effects, producing the specific periodic patterns and other particular structures, could take place in different ways in the enamel surface layers with parallel and perpendicular prisms.

But whatever the involved mechanisms could be, this is the first evidence of wave-like patterns – and in particular of resonant periodic structures – produced by laser irradiation in dental enamel and, more generally, in biological tissues. This is noteworthy because the formation mechanisms of resonant periodic structures in electroinsulating enamel should be different of those involved in the laser irradiation of conducting metals [53]. Moreover there should be a difference with respect to the generation of resonant periodic structures in electroinsulating inorganic crystals, because the very complex and hierarchical organization of enamel contrasts to the more simple and regular structure of crystals [54, 55] and of ceramic multilayered coatings [56]. However, the TEA-CO<sub>2</sub> laser irradiation by its much longer pulses provided an approach adequate to overcome these differences and produce similar effects in enamel.

#### *Quasi-disordered enamel bubbles at high fluence*

In both types of enamel, the periodic patterns evanesce and then perish towards the center of the spot, leaving place to quasi-random structures (Fig. 4A, 4B, and 5B, 5F). They do not show any more trace of periodicity and, at higher magnifications, evidence amorphous, glassy and chaotic patterns (Fig. 5C-5D and 5G-5H). They seem to be the result of more or less violent, turbulent processes of melted material boiling and evaporation due to very fast heating in the central spot zone, irradiated here by the laser beam of approximately Gaussian ( $1/e^2$ ) profile at its highest intensity.

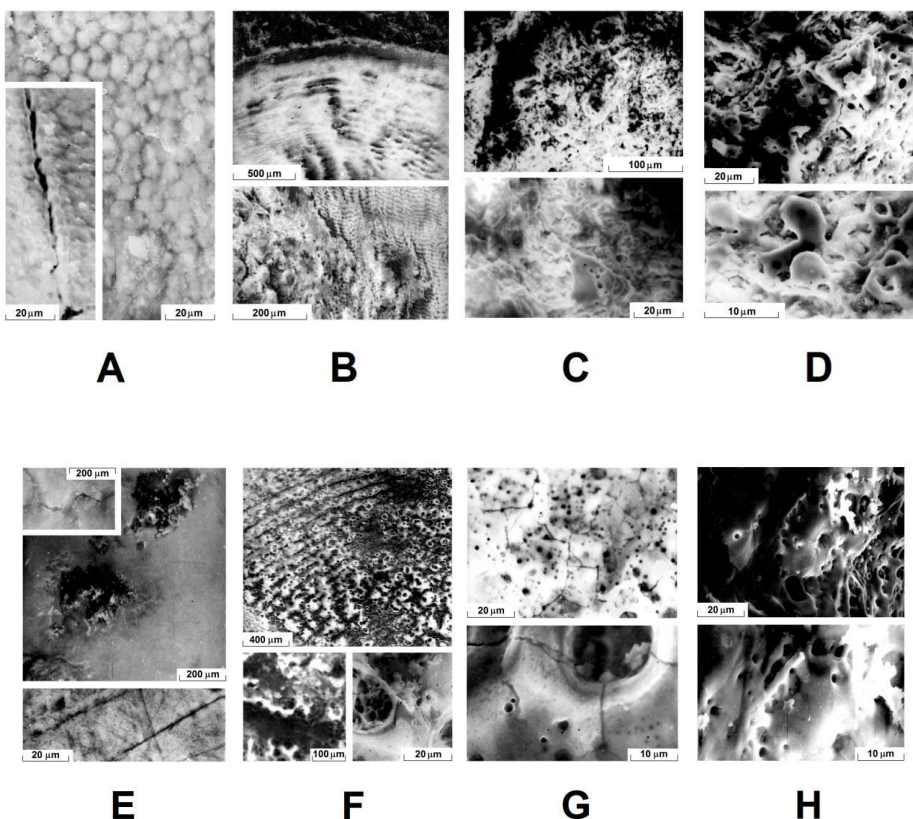


Fig. 5. SEM images of different magnifications showing normal (A, E) and irradiated (B – D and F – H) enamel at high fluence of 625 J/cm<sup>2</sup>. Enamel with perpendicular (A – D) and parallel (E – H) prisms.

The morphology of melted and disorderly resolidified enamel is different for the two types of enamel. When drawing away from the oscillatory pattern to the central area, in the enamel with perpendicular prisms the waves are steeply followed by bubbles of 50-75  $\mu\text{m}$  diameter apparently not broken (lower image of Fig. 5B). This pattern is not seen in the enamel with parallel prisms, where the concentric waves degenerate into hemispherical features of 30-100  $\mu\text{m}$  diameter and a void center with the form of broken bubbles distributed quasi-randomly (upper image of Fig. 5F). As long as they still follow the maximum of a wave, they are spaced at 30-150  $\mu\text{m}$  of each other.

At higher magnifications, the SEM appearance of the irradiated enamel with perpendicular prisms examined at various magnifications is completely "chaotic", recalling the aspect of some "boiling volcanic lava", consistent to a deeply turbulent process (Fig. 5C-5D). By contrast, the irradiated enamel with parallel prisms shows an amorphous, glassy aspect with larger cavities of 5-15  $\mu\text{m}$  and smaller cavities of  $\sim 1 \mu\text{m}$  (Fig. 5G-5H). Differences could be seen in different areas of the spot, but basically they are similar (compare the two zones presented in Fig. 5G with Fig. 5H). Although the surface is rather irregular, it may be described as "locally smooth" on a 10-40  $\mu\text{m}$  scale if we neglect the cavities.

Unexpectedly, the surface morphology of some areas of the enamel with parallel prisms irradiated with 25 pulses (Fig. 5G) and of the enamel with perpendicular prisms irradiated with 3 pulses (Fig. 3B) evidenced a similar glassy and amorphous structure in spite of the very different fluencies. This suggests most plausibly that the effective total absorbed energy was of the same order of magnitude in both cases. Thus we postulate that the enamel with parallel prisms and a small surface density of defects absorbed a smaller fraction of the energy delivered by the 25 pulses, while the enamel with perpendicular prisms and a high density of defects absorbed most of the incident energy from the 3 pulses.

Apart from providing an argument for the essential role of surface defects, this shows that the effective fluence is hard to evaluate because it depends on the surface structure of enamel. Moreover, any estimate of the effective fluence based only on the nominal fluence and on a plausibly guessed lost energy fraction due to plasma formation may be very inaccurate as long as the effects due to surface density defects are not accounted for.

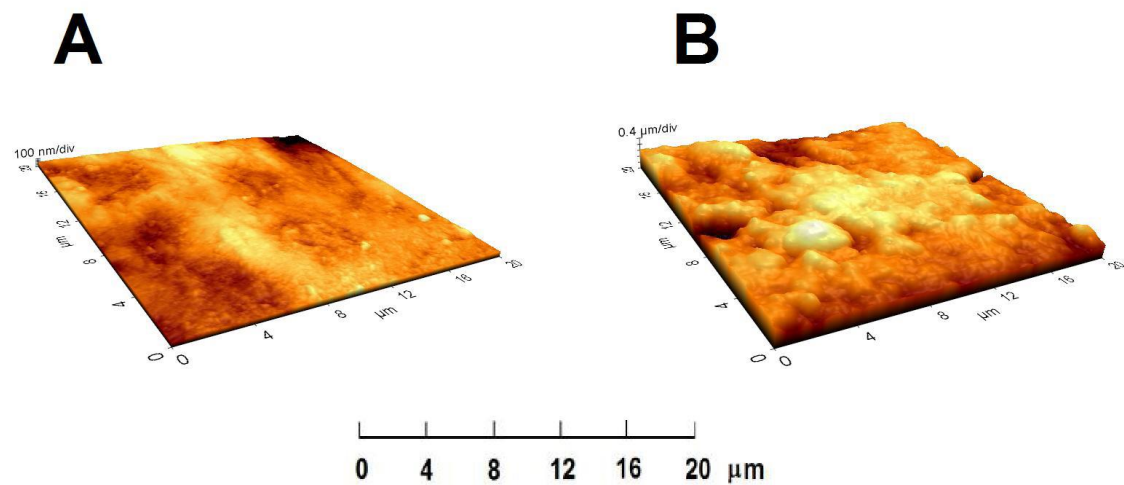


*Fig. 6. – AFM maps of enamel with perpendicular prisms of the lower molar, A – native, B – irradiated at high fluence of 625 J/cm<sup>2</sup>.*

The similar aspect of the enamel with parallel prisms irradiated with 25 pulses (Fig. 5G) and of the enamel with perpendicular prisms irradiated with 3 pulses (Fig. 3B) shows in addition fine fissures in the glassy melted substance. They formed probably by contraction-associated tensions generated by fast cooling of the melted material after each laser pulse. Thus not only the

heating was very fast ( $\sim 1 \mu\text{s}$ ) but also the cooling (although its time course was unknown). These fissures are too narrow ( $< 0.1 \mu\text{m}$ ) to accommodate bacteria, but probably they would weaken the mechanical strength of irradiated enamel.

Note finally that the AFM images of the enamel with perpendicular prisms of the lower molar (Fig. 6A) after irradiation with 25 pulses shows a ‘glassy ruggedness’ pattern (Fig. 6B) which is similar to the area scanned by SEM at a close magnification (lower image of Fig. 5D). Thus AFM evidenced also substantial ultrastructure changes with respect to the native enamel; after irradiation it displayed also small cavities of  $1\text{--}2 \mu\text{m}$  and a quasi-circular ‘bubble’-shaped detail of  $4\text{--}5 \mu\text{m}$  diameter just like the SEM image. The apparent height of the surface relief due to shadow effects in SEM images seems much higher than the AFM-measured RMS height because the field depth of SEM is much larger. Each method provided a few specific additional details with respect to the other, and confirms complementarily the ultrastructural changes induced in enamel by the laser irradiation.

#### *Fractal surface of enamel at high laser fluence*

A surprising result – mainly due to SEM’s capability of using a large range of magnifications, providing thus a comprehensive ‘big picture’ – consists in the fact that for both types of enamel, two specific and almost invariant motifs are visible on the  $10\text{--}100 \mu\text{m}$  scales in the quasi-disordered patterns produced by laser irradiation. At various magnifications and in different examined areas, the same ‘chaotic’ image was found in the case of the enamel with perpendicular prisms (Fig. 5C-5D), and the same glassy aspect was shown in the enamel with parallel prisms (Fig. 5G-5H). This suggests that in both cases the alterations had a hierarchical structure, with features which reproduced themselves approximately from lower to higher magnification. The property that a magnified view of one part will have the same qualitative appearance although it will not precisely reproduce the whole object represents precisely the so-called statistical self-similarity of natural fractals. In other words, the SEM images suggest that the surface morphology of the enamel altered by high fluence  $\text{CO}_2$  laser irradiation may have a fractal-type structure. The fractal analysis of surfaces [74] emerged as a powerful method for biomedical applications [75]. It has been applied recently in studies of dental composites [76] and allowed deeper insight in an investigation of the laser ablation of alumina [77]. The fractal dimension of patterns with rough and irregular geometric shape as those produced in enamel by laser irradiation may give a quantitative measure of complexity, defined as a change in detail with change in scale. Although the careful examination of the fractal properties of laser-irradiated enamel is beyond the scope of the present article, it is being considered in a subsequent study (Preoteasa et al, in preparation).

#### *The spot boundary at high laser fluence*

Characteristic ultrastructural configurations dependent on the orientation of the enamel prisms were observed at the boundaries of the spots produced by 25 laser pulses. The spot boundary is important because in a practical laser treatment it would be almost impossible to cover completely the surface of a tooth. It has been noted previously that the melting produced by the laser spot was not homogeneous, and was restricted to limited areas [50].

The spot of the enamel with perpendicular prisms of the lower molar shows a clear halo in certain boundary zones (Fig. 7A), while in other parts a stacked long-wavelength periodic pattern was seen, followed by a smooth but distinct outer ring (Fig. 7B). The annular moulds showed in addition short-wavelength periodic patterns (insets of Fig. 7A). Thus both forms of boundary structures exhibited definite types of order emerging just at the limit of the laser beam, which appear to be formed by solidification of melted enamel without splashing or blowing out. The halo images from the upper and lower panels of Fig. 7A displays some non-uniformity with respect to its width, varying between  $\sim 250$  and  $\sim 320 \mu\text{m}$ , and to its form. The apparent morphology differences may be explained either by genuinely different profiles of the halo in the two places, by an asymmetric profile of the halo with respect of its median, or by both. The assumption of the

halo's profile variability is favoured by its different widths from point to point. It is also substantiated by the completely different pattern in a third place on the frontier of the same spot from the lower molar as shown in Fig. 7B. In the lower panel of Fig. 7A outside calcinations of enamel are observed. The calcinations could be explained by the fact that the oscillating electromagnetic field produced inside the laser spot does not drop abruptly to zero at the periphery, but decreases exponentially outside the border [53]. A halo of about 100 µm wide surrounding the spot produced in enamel has been reported before [49]. Similarly, altered circular zones outside the laser spot were observed in a polymer film [72] and in ceramics [78]; in the latter case it was attributed to the plasma formed in the vapor plume and not to heat diffusion from the irradiation spot.

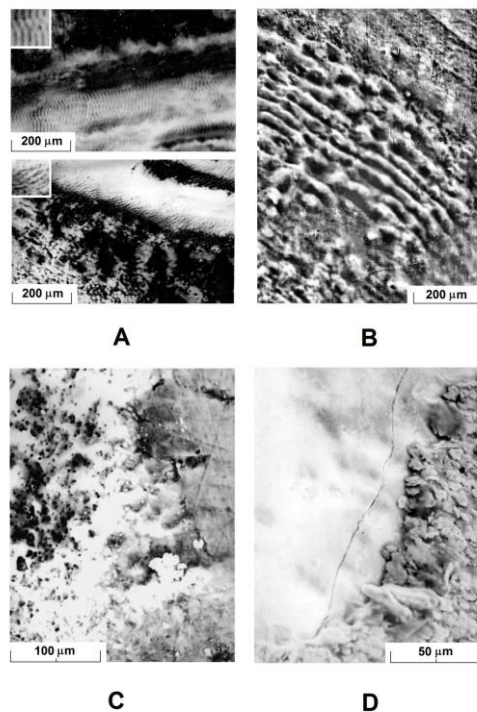


*Fig.7. – SEM images of the spot boundary in enamel with perpendicular prisms (A, B) and parallel prisms (C, D) irradiated at high fluence of 625 J/cm<sup>2</sup>. The insets in (A) show the short wavelengths periodic patterns which are superimposed on the boundary structures (enlarged twice). In (B) stacked waves are seen at the frontier. The enamel with parallel prisms shows splashed-out (C) and flaked-off(D) structures.*

In the case of the enamel with parallel prisms of the wisdom tooth the spot is bordered by dropped material. This either was melted and splashed enamel which solidified instantly taking the aspect of a foam (Fig. 7C), or ejected flaked-off debris which formed a sintered conglomerate (Fig. 7D). Both these structures seem to have been projected slightly beyond the effective limits of the radiation beam. Similarly to the splashed foam of enamel, irregular and uneven margins with complicated forms were observed at the boundaries of enamel spots [79]. The occurrence of exfoliated debris boundary structure on the enamel with parallel prisms is in agreement with the observations of other investigators [49, 50] who found flakedoff material to be more common in parallel than in perpendicular prism orientation to the specimen surface.

To conclude, the important differences evidenced between the spot border effects produced on enamel with perpendicular and parallel prisms strongly supports the postulate that certain ablation mechanisms involved were different as a function of enamel prisms orientation with respect to the tooth surface.

#### *Laser ablation of cementum and cementoenamel junction*

The SEM examination of the laser-irradiated cementum (Fig. 8) shows more devastating effects as compared to enamel. This is most strikingly seen in the case of the lower molar, where the cervical cementum below the cementoenamel junction was vigorously ablated resulting in the deepest crater of all irradiated specimens, of a few tenths of millimeter (Fig. 1B). The difference to enamel is explained by the very different composition of cementum: approximately 45-50% inorganic material (mainly hydroxyapatite), 33% organic material (mainly collagen) and 17-22% water, as compared to about 96% inorganic material in enamel. The relatively large amount of water retained in the highly porous structure evaporated instantaneously causing a *hydrokinetic ablation* of the first layers of cementum. This has been observed in fact during the laser irradiation as a microexplosion with expulsion of debris. It was a particular case of laser-induced explosion of solids [80].

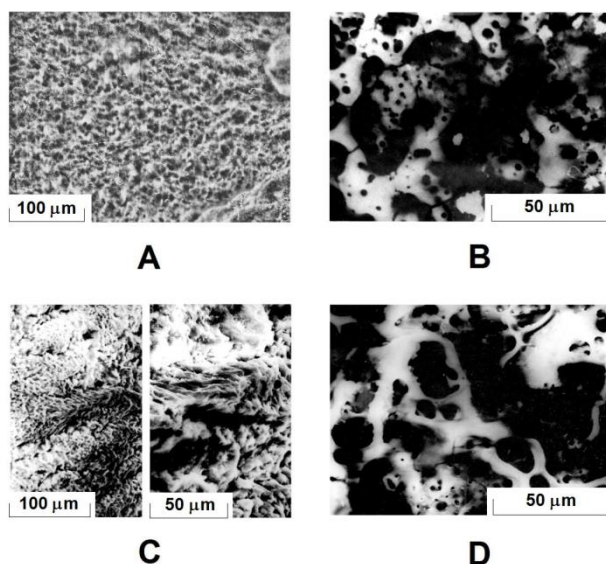


Fig. 8. – SEM images of native cementum from the upper incisor (A) and lower molar (C), and of cementum of these teeth irradiated with  $75 \text{ J}/\text{cm}^2$  (B) and  $625 \text{ J}/\text{cm}^2$  (D).

The native dental cementum has a loose and fibrous morphology forming a network with irregular surface. We observed this network either as a disordered and isotropic structure as in the central incisive (Fig. 8A) or as somewhat anisotropic with fibers partly oriented along a preferential direction and many canals connecting lacunary spaces in the lower molar (Fig. 8C). After irradiation with 3 pulses of the central incisive and 25 pulses of the lower molar, respectively, the surface morphology could hardly be recognized (Fig. 8B and 8D). Both types of cementum showed structures which suggest a massive melting of the mineral substance followed by resolidification in an amorphous glassy architecture with large alveoli ( $\sim 10\text{--}40 \mu\text{m}$  diameter) and pores ( $\sim 1\text{--}5 \mu\text{m}$  diameter).

The alterations of cementum were less extensive in studies using different types of lasers with milder irradiation conditions. The CW irradiated cementum was described as micro-irregular and particulate with numerous projections [81], while pulse irradiation produced a low depression of round shape, circular borders and irregular adjacent area [82]. Pulsed irradiation at subablative fluences of  $25\text{--}35 \text{ J}/\text{cm}^2$  resulted in a uniform melting without the presence of superficial ablation [83]. But although we used higher fluences, no cracking was observed in the melted cementum, as noted in different circumstances [81].

There are certain differences between the two cementum surfaces irradiated with different fluencies: the cavities are significantly larger after 25 than after 3 pulses, and the solid glassy network which demarcate the voids are bigger and sparser. The different structures of the native

cementum in the two irradiated areas and the different laser fluences could be easily invoked to explain the disparities between the two irradiated cementum areas (Fig. 8B and 8D).

However the resemblances of the alterations induced in the two cements were considerable although irradiated with different fluencies (Fig. 8B and 8D). This behavior was in contrast to that of enamel and seemed more difficult to understand at first sight. One possible explanation could be the saturation of the laser effects after a few pulses. For another possible interpretation we postulate that the energy carried by the 25 pulses was only partly used for melting the cementum of the lower molar, because an important fraction was used for the hydrokinetic ablation of the first layers of cementum. This would reduce the difference between the energy delivered to the cementum for shaping the final morphology in the lower molar (25 pulses) and the central incisive (3 pulses) and, accordingly, the final alterations were comparable. On the basis of the present data, we cannot decide in favour of one hypothesis or the other, or of both.

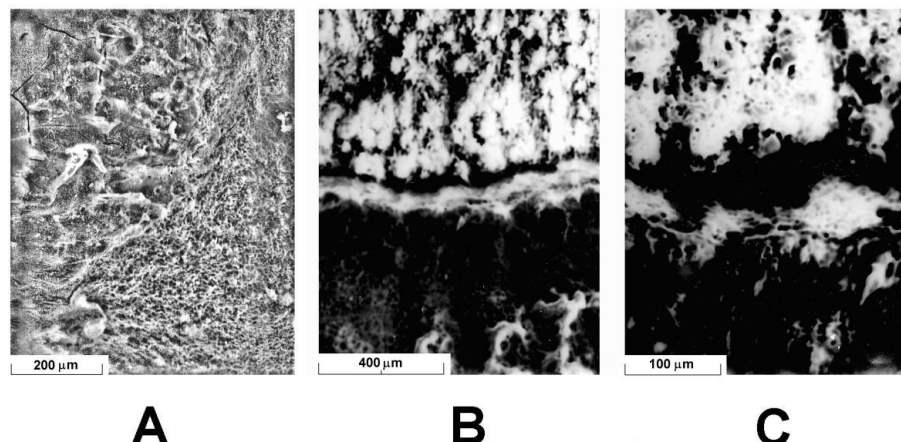


*Fig. 9 – SEM images of cementoenamel junction (CEJ) in native state with enamel in upper left area and cementum in lower right zone (A) and CEJ irradiated with 625 J/cm<sup>2</sup> shown at different magnifications (B, C), with enamel above and cementum below.*

The native cementoenamel junction of the upper incisor illustrates a less compact and naturally fissured structure of enamel and the fibrous aspect of cementum, without a specific barrier element between them (Fig. 9A). The cementoenamel junction of the lower molar located at the center of the spot irradiated with 25 laser pulses (Fig. 9B and 9C) shows three distinct regions: 1) the melted enamel structure similar to the irradiated enamel far from the junction but less compact (Fig. 5); 2) the damaged (ablated) and melted cementum similar to Fig. 8D; and 3) an interface zone consisting in a narrow groove in the enamel region, a larger groove in the cementum region apparently depleted of much of the cementum, and a ‘wall’ looking like melted enamel in the middle. Some parts of this ‘wall’ show discontinuities at a higher magnification (Fig. 9C). Note that the enamel itself shows grooves and channels absent in the irradiated bulk enamel zones. The overall aspect indicates a rather sensitive, even vulnerable zone of the teeth which undergoes most drastic effects induced by laser irradiation.

#### *Laser-irradiated enamel surface roughness evaluated by AFM*

Quantitative characterization of laser-induced changes of enamel was allowed by AFM measurement of surface roughness assessed by its root mean square (RMS). This makes possible concomitant correlations involving different enamel areas and teeth irradiated with 0, 3, 7 and 25 pulses. Mean values of about 66, 324, 358 and 232 nm were estimated for RMS at 0, 75, 175 and 625 J/cm<sup>2</sup> nominal fluence, showing a roughly increasing trend with the surface energy density

followed by saturation. These RMS values are rather small and they describe only the local roughness as seen in the  $20 \times 20 \mu\text{m}^2$  AFM maps.

Although we did not perform an accurate examination of the roughness-fluence relationship and the available data are rather scarce, together with a few prerequisites they afford at last a semi-quantitative image. First, we assume a threshold fluence of  $13 \text{ J/cm}^2$  where the first ultrastructural changes appear [6]. Moreover, this is supposed to be the highest fluence which produces a practically negligible effect on enamel and thus the corresponding RMS roughness is presumed to be the same as in the control enamel. Accordingly, the data points representing the roughness  $R$  dependence on fluence  $\sigma$  are consistently fitted above the threshold  $\sigma_c$ , in particular with an exponential saturation curve or with a Langmuir function typical for surface adsorption-desorption phenomena (Fig. 10):

$$R = \begin{cases} R_0 = \text{const.}, & \text{for } \sigma \leq \sigma_c \\ R_0 + (R_{max} - R_0) \left[ 1 - \exp \left( -\frac{\sigma - \sigma_c}{s} \right) \right], & \text{or} \\ \frac{R_{max} b \sigma^{1-c}}{1 + \sigma^{1-c}}, & \text{for } \sigma > \sigma_c \end{cases} \quad (1)$$

where  $\sigma_c$  is the fluence threshold given in nm as long as  $\sigma$  and  $R$  is given in  $\text{J/cm}^2$ .

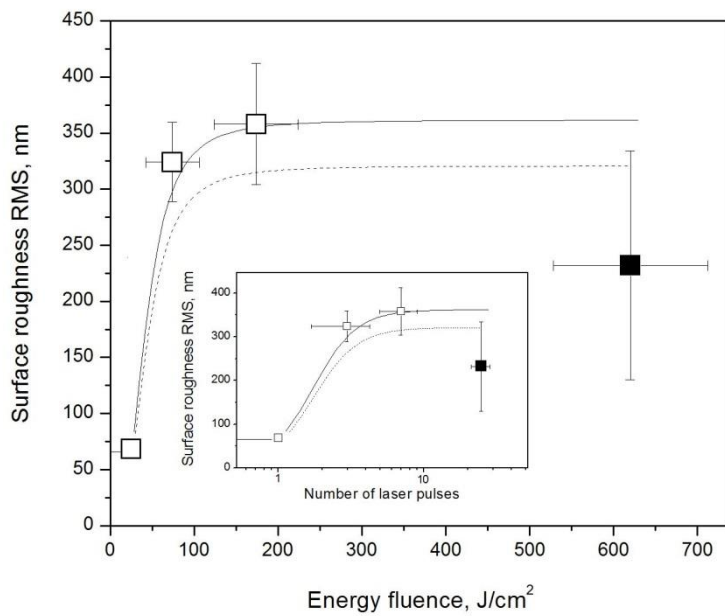


*Fig. 10. Illustration of the dependence on laser fluence of the AFM-measured RMS roughness of irradiated enamel with perpendicular prisms. Open squares and solid line, upper incisor with ordered prisms. Full square, lower molar with disordered prisms. The open and full squares were included together in the fit with the dashed line. The fit curves are Langmuir functions. The inset shows a semilogarithmic plot as a function of number of pulses.*

In the exponential function  $R_0$  is the rugosity in the absence of laser irradiation,  $R_{max}$  is the maximum (saturation) rugosity produced by laser, and  $s$  is a saturation constant with the dimension of fluence. In the Langmuir function  $R_{max}$  has the same meaning as above while  $b$  and  $c$  are parameters. Taking  $\sigma_c = 13 \text{ J/cm}^2$  for the critical fluence one finds  $R_{max} \approx 360 \text{ nm}$  for the upper central incisive alone and  $R_{max} \approx 320 \text{ nm}$  if the data of the incisive and of the lower molar are pooled and fitted together. Of course, similar values for  $R_{max}$  are obtained if another threshold is chosen, e.g.  $\sigma_c = 30 \text{ J/cm}^2$  which slightly above the value of  $25 \text{ J/cm}^2$  where the first macroscopic

changes appear [6]. The dependence of the saturation  $R_{max}$  on the inclusion of the molar in the fit highlights the significantly different response of this tooth's enamel as compared to the incisive's enamel, although the enamel had perpendicular prisms in both teeth. This suggests that besides the orientation of prisms with respect to the surface, other structural factors – size and form of prisms, crystallinity and interprism enamel filling the volume between prisms – should play a role in the effects of laser irradiation. The lower value of the molar's  $R_{max}$  may be due to the closer packing of prisms and lower amount of interprism enamel in the molar than in the incisor because the same laser energy has to ablate a larger amount of enamel in its hardest crystallized form in a surface layer of a similar thickness. Although the experimental errors were considerable, this hypothesis remains plausible and worth of further investigation.

The shape of the curves shown in Fig. 11 and described by eq. (1) is similar to the fluence dependencies of other effects in laser ablation which show also an initial lag and increase above a threshold reaching asymptotically a saturation. Thus the desorption yield of ions of different masses from dentin irradiated with a free electron laser (FEL) increases with the fluence above a threshold and then saturates [84]. Similar curves have been obtained for the ablation rate of enamel and dentin [40], for cut depth in bone [85, 21], and for ablation rate of ceramics, aluminum and steel [78]. Also, the quasi-unidimensional flowing thickness of the vapour-plasma mixture produced in the ablation of aluminum by a CO<sub>2</sub> laser appears to increase above a threshold and, even if it did not reach saturation in the investigated fluence domain, its derivative decreased monotonously [86], similarly to the initial branches of our curves. Let apart the occurrence of a threshold which was to be expected in our experiment, the significance of the mentioned similarity is still unclear, but it suggests that the laser action on enamel has a common nature with other laser ablation processes. It may also involve a contribution related to the fluence dependence of plasma formation, as suggested by the second comparison. Further studies could be devised to examine this suggestion.

#### *Potential for hard dental tissue procedures*

The effects produced in the low fluence domain are of high interest because here the CO<sub>2</sub> laser – delivering the energy of short pulses to a small volume at the surface of enamel with less risk of damages in dental pulp (review in [73]) – is the most successful laser for increasing enamel's resistance to caries by reducing the rate of subsurface enamel demineralization [25, 73, 87]. The CO<sub>2</sub> laser irradiation „can reduce initial enamel demineralization, inhibit subsequent lesion progression, and enhance fluoride adsorption” [73]. At 10.6 μm which is the strongest line of the CO<sub>2</sub> laser and fluences from 2 to 50 J/cm<sup>2</sup> without fluoride, the caries inhibition varied between 30 to 55 % and better [6, 24, 87, 88]. For prophylactic action the 10.6 μm CO<sub>2</sub> laser was superior to the Nd:YAG laser and comparable to the Er:YAG and Er,Cr:YSGG lasers with a 40 % and 60 % maximum caries reduction, respectively [73, 89]. We investigated the changes induced in the enamel surface ultrastructure, but keeping in mind that the effects at various levels (surface landscape, crystallographic, chemical and elemental) are much more complex.

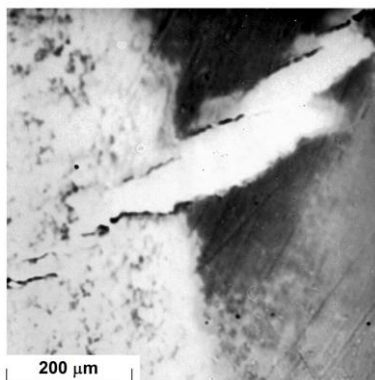


*Fig. 11. A large fissure in enamel protruding in the spot (left side) was not sealed by laser irradiation at low fluence of 75 J/cm<sup>2</sup>.*

At the lowest tested fluence of 75 J/cm<sup>2</sup> the uniform glazing of enamel with minimal physiognomic changes may be well suited for increasing resistance to demineralization and caries prevention [41, 87]. In particular, the ~2 μm spaces between the perpendicular prisms filled with the less ordered interprismatic enamel were completely sealed even at this low fluence, which provided thus an adequate protective effect. The results suggest future tests of fluoride [32 – 34], bioglass [30] or hydroxyapatite [35, 90] capping of enamel combined with the TEA-CO<sub>2</sub> laser, in search for better results than e.g. with the argon laser which increases fluoride uptake by photochemical action [73, 91].

Special care is needed however at the margins of the spot where splashed or flaked-off material and adjacent calcinations may occur and host plaque and bacteria favoring thus subsequent caries onset. Moreover note that at the boundary of the spot, where the Gaussian beam profile provides a relatively low intensity ( $\sim 1/e^2$ ), the large enamel fissures or other defects are not sealed due to the low average fluence of 75 J/cm<sup>2</sup> (Fig. 11) and thus the irradiation yields only a limited protection against caries at the boundary of the spot in these conditions.

Considering the irradiation of cementum, it is encouraging to note that at the low fluence corresponding to 3 pulses the cementum was melted superficially but was not damaged by hydrokinetic ablation as with 25 pulses. Therefore the low fluence may be tested also for treatments of lesions in chronic periodontitis such as scaling of periodontal pockets [92]. Also, given that the excellent performances of the CO<sub>2</sub> laser for soft tissues may be used for the healing of periodontal wounds [93], the lack of cementum damage at low fluence implies that the unintended but sometimes unavoidable irradiation of the tooth below the cementoenamel junction during such treatments will not be harmful.

The cementum is however strongly damaged and deeply ablated by the hydrokinetic mechanism, and the roughness in the cementoenamel junction region is increased at the highest tested fluence of 625 J/cm<sup>2</sup> (25 pulses). This strongly recommends caution and milder laser treatments, e.g. about 75 J/cm<sup>2</sup> near the gingiva with the irradiation limited as much as possible to enamel, because the damaged hard tissues in this region will obviously favor caries onset by hosting plaque and bacteria.

Also, the purely thermal ablation with a depth of 25 – 100 μm produced in enamel at 625 J/cm<sup>2</sup> fluence is too low for caries treatment and cavity preparation.

But in enamel the unexpectedly observed – and remarkable – periodic patterns and the quasi-disordered bubbles generated at 625 J/cm<sup>2</sup>, which are characterized by a gross surface roughness of about 10 – 50 μm, could be ideal for increasing the bond strengths of composite materials to enamel and thus extend the lifetime of dental restorations. A similar effect could be obtained at the intermediate fluence of 175 J/cm<sup>2</sup> which produced a flaked-off surface of enamel by exfoliation of the hydroxyapatite crystals, but the mechanical strength could be lower in this case because the bonding of the sintered ablation products to the bulk enamel could be weaker as compared to the waves and bubbles. In a previous study, CO<sub>2</sub> laser irradiation induced

significantly higher bond strength of bioglass [30] and ceramics composites [31] to dentin. Such a laser treatment may be applied for instance to the surface of drill prepared cavities, as an alternative to the classical roughening by phosphoric acid etching. Moreover, it may find an excellent, simple and new application, without need of previous drill treatment, for the protective sealing of the molars' grooves with fluid composite restoration materials, e.g. for patients complaining of hypersensitivity to cold and hot fluids.

The strong dependence of the effects produced by the TEA-CO<sub>2</sub> laser in enamel on the orientation of prisms means, from a practical point of view, that a precise and reproducible treatment is not possible unless the later is well known. This is a difficult task because the prisms' orientation may vary from one tooth to another and from cusp to cusp. For now we could consider only two approaches of this problem. On one hand, one should have a complete map of prism orientation in all teeth, but this is not feasible due to the biological individual variability. On the other, the determination of prism orientation should require an *a priori* examination of the enamel surface, for instance with some optical reflection microscope or with an optical device for the diagnosis of prisms orientation based on their anisotropy [47]. Without a specially designed optical sensor this would be hard to perform *in situ* in the general dental surgery. Therefore further studies of the enamel surface anisotropy effects in laser irradiation – largely ignored before with a few exceptions [48 – 50] –, as well as for the engineering of a dedicated enamel prism orientation diagnosis device, are necessary for a better understanding and control of these effects.

#### **4. Conclusions**

The TEA-CO<sub>2</sub> laser pulses ~2 μs long at fluences above the macroscopic changes threshold and at low repetition rate produced a large variety of ultrastructural effects in enamel and cementum as evidenced by SEM and AFM. The most striking change was the generation of periodic ablation patterns in enamel at 625 J/cm<sup>2</sup>, reported here for the first time in a biological hard tissue. The period of the ‘frozen waves’ was of  $42 \pm 2 \mu\text{m}$  in the enamel with perpendicular prisms, while in the tooth with parallel prisms it was of  $68 \pm 7 \mu\text{m}$ . Moreover, the enamel with perpendicular prisms showed shorter periodic structures of  $11.0 \pm 1.5 \mu\text{m}$  which were absent in the enamel with parallel prisms. The later short waves showed the characteristics of ‘resonant periodic structures’ seen before in non-biological materials such as metals, dielectric crystals and ceramic multilayered coatings. The dependence of AFM-measured roughness on fluence showed a threshold and an asymptotic saturation in the irradiated enamel with perpendicular prisms. Thus the observed effects were dependent not only on fluence but also on the orientation of enamel prisms, as well as on the density of surface defects. Such characteristics appear to play an important role in the differences evidenced between the dental targets with different surface structure.

The potential of the results may suggest beneficial applications in dentistry, both along the traditional lines, e.g. caries prevention at 75 J/cm<sup>2</sup>, as well as in the perspective of new practical uses at 175 and 625 J/cm<sup>2</sup>. A possible new application could make use of the surface roughness of (probably) about 10 – 50 μm associated to the periodic patterns and the bubbles with fractal-like structure produced in enamel at 625 J/cm<sup>2</sup>, and to the flaked-off surface generated at the intermediate fluence of 175 J/cm<sup>2</sup>. This surface roughening could improve the bond strengths of composite materials adhesion to enamel both in drill prepared cavities and on the molar grooves sealed with fluid composites for protection. In the later application suggested here, the roughened enamel surfaces pertain to hidden locations on the teeth so that no possible physiognomic inconvenience is entailed. On the other hand, treatments of periodontitis should use low fluences around 75 J/cm<sup>2</sup>, which melt superficially the cementum without producing gross damage by hydrokinetic ablation. The results emphasize the role of the local structure of enamel and of its hierarchical organization typical for biological materials. The ablation patterns produced in enamel at 625 J/cm<sup>2</sup> by the TEA-CO<sub>2</sub> laser were proven to be dependent on the orientation of prisms, which should be known prior to irradiation for a precise and reproducible treatment. So far, a method for the determination of this microanatomical parameter *in situ* is not at hand, and the

statistical spread of the effects is high due to various prism orientation and to plasma formation characteristic to the TEA-CO<sub>2</sub> laser. Thus further studies for the evaluation of enamel surface anisotropy and its role in laser irradiation are needed.

Both the SEM and AFM microscopy results reveal the necessity of continuing the studies of teeth hard tissue irradiation with TEA-CO<sub>2</sub> lasers in more controlled experimental conditions and using different pulse parameters. Studies of the plasma plume may help for a more accurate evaluation of the effective fluence delivered to the tooth hard tissues. In addition to the 10.6 μm radiation, the other wavelengths of the CO<sub>2</sub> lasers (9.3, 9.6, 10.3 μm) should be explored because they have different absorption coefficients in the two main components of the hard tissues – hydroxyapatite and water. This may help augmentation of desired effects and reduction of damaging ones. Measurements of surface optical characteristics of dental enamel could help the determination of the prisms orientation and may lead the way for the engineering of a diagnosis device for clinical applications. Finally, in addition to SEM and AFM, there are many atomic and nuclear surface analysis methods which could characterize the physical and chemical effects produced by the TEA-CO<sub>2</sub> laser.

In brief, our SEM and AFM studies may be considered only a first step, at the ultrastructural level, in the characterization of the effects determined in enamel and cementum by the TEA-CO<sub>2</sub> laser. More important, we succeeded to evidence certain ablation patterns dependent on enamel's prisms orientation, and especially periodic structures which were not reported in previous investigations. In the second part of this study, simple physical models are postulated to allow a better interpretation of the laser-enamel interactions beyond the micro- and ultrastructural appearance.

### Acknowledgement

The authors express their sincere regrets for the disappearance of Drs. V. Tatu and I. Patru, departed before the preparation of this article. Their participation in the experimental work and their valuable suggestions, together with those of Dr. C. Grigoriu, are gratefully appreciated.

### References

- [1] R.A. Convissar, Principles and Practice of Laser Dentistry. Mosby Elsevier, St Louis, MO (2010)
- [2] L.J. Miserendino, R.M. Pick (Editors), Lasers in Dentistry, Quintessence Publishing Co. Inc., Hanover Park, IL. (1995)
- [3] A. Hussein, (Review), Archives of Orofacial Sciences **1**, 1-4 (2006)
- [4] L.J. Walsh, (Review), Australian Dental Journal **48**, 146-155 (2003)
- [5] D.J. Coluzzi, (Review), J. Laser Dentistry **16** (Spec issue), 4-10 (2008)
- [6] R.H. Stern, J. Vahl, R.F. Sognnaes, J. Dent. Res. **51**, 455-460 (1972)
- [7] R.A. Convissar, (Review), Wisdom **11**, 8-10 (2011)
- [8] Academy Report, (Review), J. Periodontol. **73**, 1231-1239 (2002)
- [9] N. Gutknecht, (Review), J. Laser Health Acad. No. 3/1, 1-5 (2008); [www.laserandhealth.com](http://www.laserandhealth.com)
- [10] G. Romanos, H.-H. Ko, S. Froum, D. Tarnow, Photomed. Laser Surg. **27**, 381–386 (2009)
- [11] J. Melcer, Rev. Stomat. Chirur. Maxilofac. **83**, 146-151 (1982)
- [12] J. Melcer, F. Melcer, R. Hassen, J. Gauthier, Rev. d'Odonto-Stomatol. **11**, 351-355 (1982)
- [13] P. Viraparia, J.M. White, R.M. Vaderhobli, in: CO<sub>2</sub> Laser - Optimisation and Application, (Edited by D.C. Dumitras), InTech, Rijeka (Croatia)-New York-Shanghai (2012)
- [14] H.A., Wigdor, J.T. Walsh Jr., J.D. Featherstone, S.R. Visuri, D. Fried, J.L. Waldvogel, Lasers Surg. Med. **16**, 103-133 (1995)
- [15] A. Obata, T. Tsumura, K. Niwa, Y. Ashizawa, T. Deguchi, M. Ito, Eur. J. Orthod. **21**, 193-198, (1999)
- [16] G. Sun, Dent. Clin. North Am. **44**, 831-850 (2000).

- [17] J.D. Featherstone, Dent. Clin. North Am. **44**, 955-969 (2000)
- [18] L.W. Seldin, Future of Dentistry: Today's Vision: Tomorrow's Reality, American Dental Association, Health Policy Resources Center (2001).
- [19] R. Mullejans, G. Eyrich, W.H. Raab, M. Frentzen, Lasers Surg. Med. **30**, 331-336 (2002)
- [20] D. Brune, Scand. J. Dent. Res. **88**, 301-305 (1980)
- [21] M.M. Ivanenko, T. Mitra, P. Hering, SPIE Proc. Optical Biopsy and Tissue Optics **4261-08** (2000)
- [22] M. Pao-Chang, X. Xion-Qui, Z. Hui, L. Zheng, Z. Rui-Peng, Laser Surg. Med. **1**, 375-384 (1981)
- [23] S.M. McCormack, D. Fried, J.D.B. Featherstone, R.E. Glena, W. Seka. J. Dent. Res. **74**, 1702-1708 (1995)
- [24] J.D.B. Featherstone, N.A. Barrett-Vespone, D. Fried, Z. Kantorowitz, W. Seka, J. Dent. Res. **77**, 1397-1403 (1998)
- [25] Z. Kantorowitz, J.D. Featherstone, D. Fried, J. Am. Dent. Assoc. **129**, 585-591 (1998)
- [26] J.D.B. Featherstone, D.G.A. Nelson, Adv. Dent. Res. **1**, 21-26 (1987).
- [27] Y. Launay, S. Mordon, A. Cornil, J.M. Brunetaud, Y. Moschetto, Laser Surg. Med. **72**, 472 (2008)
- [28] M. Staninec, C.L. Darling, H.E. Goodis, D. Pierre, D.P. Cox, K. Fan, M. Larson, R. Parisi, D. Hsu, S.K. Manesh, C. Ho, M. Hosseini, D. Fried, Lasers Surg. Med. **41**, 256-63 (2009)
- [29] R. Merard, Inf. Dent. **64**, 2153-2157 (1982)
- [30] A.S. Bakry, H. Takahashi, M. Otsuki, A. Sadr, K. Yamashita, J. Tagami, J. Dent. Res. **90**, 246-250 (2011)
- [31] B. Ersu, B. Yuzugullu, A. Ruya Yazici, S. Canay, J. Dent. **37**, 848-856 (2009)
- [32] X.-L. Gao, J.-S. Pan, C.-Y. Hsu. J. Dent. Res. **85**, 919-923 (2006)
- [33] C.-Y.S. Hsu, T.H. Jordan, D.N. Dederich, J.S. Wefel, J. Dent. Res. **80**, 1797-1801 (2001)
- [34] K. Müller-Ramalho, C. de Paula Eduardo, N. Heussen, R. Garcia Rocha, F. Lampert, C. Apel, M. Esteves-Oliveira, Lasers Med. Sci. **28**, 71-78 (2013)
- [35] L. Stewart, G.L. Powell, S. Wright, Operative Dentistry **10**, 2-5 (1985)
- [36] C.B. Gimbel, Dent. Clin. North Am., **44**, 931-953 (2000).
- [37] M.H. Niemz, Laser-Tissue Interactions: Fundamentals and Applications, Springer-Verlag, Berlin Heidelberg New York (1996)
- [38] A. Sagi, T. Segal, J. Dagan. Mathematical Biosciences 71(1), Sep 1984, 1-17
- [39] M. Jaunich, S. Raje, K. Kim, K. Mitra, Z. Guo, Int. J. Heat Mass Transfer **51**, 5511-5521 (2008)
- [40] J. Neev, J. Squier. SPIE Proceedings Applications of Ultrashort-Pulse Lasers in Medicine and Biology, (Joseph Neev, Editor) **3255**, 105-115 (1998)
- [41] M.H. Niemz. in SPIE Proc. Applications of Ultrashort-Pulse Lasers in Medicine and Biology, (Joseph Neev, Editor) **3255**, 84-91 (1998)
- [42] M.M. Ivanenko, G. Eyrich, E. Bruder, P. Hering, Lasers Life Sci. **9**, 171-179 (2000)
- [43] M. Gantri, H. Trabelsi, E. Sediki, R. Ben Salah, J. Biophys. **2010**, Article ID 253763, 9 p. (2010)
- [44] S.L. Jaques, S.A. Prahl, Laser Surg. Med. **6**, 494-503 (1987)
- [45] E.A. Preoteasa, E. Preoteasa, A. Kuczumow, D. Gurban, L. Harangus, D. Grambole, F. Herrmann. X-Ray Spectrom. **37**, 517-535 (2008)
- [46] T. Zeygerson, P. Smith, R. Haydenblit, Arch. Oral Biol. **45**, 1091 (2000)
- [47] G. Duplain, R. Boulay, P.A. Bélanger. Appl. Optics **26**, 4447-4451 (1987)
- [48] S.M. Nomelini, A.E. Souza-Gabriel, M.A. Marchesan, M.D. Sousa-Neto, Y.T. Silva-Sousa, Microsc. Res. Tech. **72**, 737-743 (2009)
- [49] M.K. Yamada, M. Uo, S. Ohkawa, T. Akasaka, F. Watari, Mater. Transact. **45**, 1033-1040 (2004)
- [50] J.M. Ferreira, J. Palamara, P.P. Phakey, W.A. Rachinger, H.J. Orams, Arch. Oral. Biol. **34**, 551-562 (1989)
- [51] M.H. Niemz, L. Eisenmann, T. Pioch, Schweiz. Monatsschr. Zahnmed. **103**, 1252-1256 (1993)

- [51] M. Frentzen, C. Winkelsträter, H. van Benthem, H.J. Koort, Dtsch. Zahnärztl. Z. **49**, 166-168 (1994)
- [53] A.M. Prokhorov, V.I. Konov, I. Ursu, I.N. Mihailescu, Laser Heating of Metals, Adam Hilger, Bristol-Philadelphia-New York (1990)
- [54] P.A. Temple, M.J. Soileau, IEEE J. Quant. Electron. **QE-17**, 2067 (1981)
- [55] F. Keilmann, Y.H. Bai, Appl. Phys. **A 29**, 9, 1982
- [56] B. Gakovic, C. Radu, M. Zamfirescu, B. Radak, M. Trtica, S. Petrovic, P. Panjan, C. Ristoscu, I.N. Mihailescu, F. Zupanic. Surf. Coat. Technol. **206**, 411–416 (2011)
- [57] D. Fried, T.M. Breunig, Lasers in Dentistry VII, Vol. **4249**, 99-104 (2001)
- [58] E.P. da Silva Tagliaferro, L.K. Rodrigues, L.E. Soares, A.A. Martin, M. Nobre-dos-Santos, Photomed. Laser Surg. **27**, 585-590 (2009)
- [59] A.J. Welch, J.H. Torres, W.-F. Cheong, Texas Heart Inst. J. **16**, 141-149 (1989)
- [60] B. Payne, The role of chromophore on pulsed laser ablation of biological tissues, Thesis, Univ. Denver (1994)
- [61] I. Apostol, D. Dragulinescu, C. Grigoriu, I.N. Mihailescu, V.S. Tat, Rom. Rep. Phys. (Stud. Cerc. Fiz.) **28**, 163-180 (1976) [in Romanian]
- [62] H.M. Lamberton, R.P. Pearson, Electronics Lett. **7**, 141 (1971)
- [63] P. R. Pearson, H. M. Lamberton, IEEE J. Quantum El. **QE-8**, 145-149 (1972)
- [64] I.N. Mihailescu, I. Neda-Apostol, I.M. Popescu, V.S. Tat, Rev. Roum. Phys. **18**, 137-139 (1973)
- [65] A.I. Ciura, E. Cojocaru, C. Grigoriu, I.M. Popescu, V.G. Velculescu, Rev. Roum. Phys. **17**, 387-388 (1972)
- [66] I. Apostol, L.C. Arsenovici, I.N. Mihailescu, I.M. Popescu, I.A. Teodorescu, Rev. Roum. Phys. **20**, 655-659 (1975)
- [67] C. Grigoriu, H. Brinkschulte, Phys. Lett. **42**, 347 (1973)
- [68] M. Esteves-Oliveira, D.M. Zezell, J. Meister, R. Franzen, S. Stanzel, F. Lampert, C.P. Eduardo, C. Apel, Caries Res. **43**, 261-268 (2009)
- [69] C. Steiner-Oliveira, L.K.A. Rodrigues, L.E.S. Soares, A.A. Martin, D.M. Zezell, M. Nobre-Dos-Santos, Dental Mater. J. **25**, 455-462 (2006)
- [70] C.L. Darling, D. Fried. Optics Express **16**, No. 4, 2685–2693, 18 February 2008
- [71] M. Esteves-Oliveira, Wirkung verschiedener Parameter der CO<sub>2</sub>-Laserstrahlung bei der Entmineralisierung des Rinderzahnschmelzes, Thesis, Techinsche Hochschule, Aachen (2008)
- [72] D.W. Zeng, K.C. Yung, Appl. Surface Sci. **180**, 280-285 (2001)
- [73] P.A. Ana, L. Bachmann, D.M. Zezell, (Review), Laser Phys. **16**, 865–875 (2006)
- [74] J.C. Russ, Fractal Surfaces, Springer-Verlag, Berlin-Heidelberg-New York (1994)
- [75] G.A. Losa, T.F. Nonnenmacher, Fractals in Biology and Medicine, Vol. **4**, Springer-Verlag, Berlin-Heidelberg-New York (2005)
- [76] M. Salerno, L. Giacomelli, G. Derchi, N. Patra, A. Diaspro, BioMed. Engn. OnLine **9**, 1-11 (2010)
- [77] S.P. Harimkar, N.B. Dahotre, Mater. Charact. **59**, 700 – 707 (2008)
- [78] S.V. Garnov, V.I. Konov, T. Kononenko, V.P. Pashinin, M.N. Sinyavsky, Laser Phys. **14**, 910–915 (2004)
- [79] K. Nagai, J.-I. Kinoshita, Y. Kimura, K. Matsumoto, J. Oral Laser Applic. **6**, 265-276 (2006)
- [80] J.C. Koo, J. Appl. Phys. **48**, 618-650 (1977)
- [81] K.M. Sasaki, A. Aoki, S. Ichinose, I. Ishikawa, Lasers Surg. Med. **31**, 79-85 (2002)
- [82] I.-S. Watanabe, R.A. Azeredo, E.A. Liberti, A.N. Sobrinho, S. Goldenberg, Rev. Odont. UNESP (São Paulo) **15/16**, 91-98 (1986/87)
- [83] L. Bachmann, W. Rossi, D.M. Zezell. J. Laser Applic. **16**, 193-195 (2004)
- [84] S. Ogino, K. Awazu, Nucl. Instrum. Methods Phys. Res. **B 144**, 236-239 (1998)
- [85] M.M. Ivanenko, P. Hering. SPIE Proc. Thermal Therapy, Laser Welding and Tissue Interaction **3565**, 110-115 (1998)
- [86] M. Stoica, D. Craciun, I.N. Mihailescu, 136-151 in: Laser Research and Engineering (V. Vasiliu, editor), Central Institute of Physics, Bucharest-Magurele (1989)
- [87] D.G. Nelson, W.L. Jongbloed, J.D. Featherstone, New Zealand Dent. J. **82**, 74 (1986).

- [88] M.N. Santos, J.D.B. Featherstone, D. Fried, Proc. SPIE **4249**, 169 (2001).
- [89] J. Hadley, D.A. Young, L.R. Eversole, J.A. Gornbein. J. Am. Dent. Assoc. **131**, 777-785 2000
- [90] M.H. Niemz, Appl. Phys. **B 58**, 493-499 (1994)
- [91] G. Demortier, S. Nammour, Nucl. Instrum. Methods Phys. Res. **B 266**, 2408–2411 (2008)
- [92] A. Miyazaki, T. Yamaguchi, J. Nishikata, et al., J. Periodontol **74**, 175-180 (2003)
- [93] C.J. Arcoria, R.E. Steele, B.A. Vitasek, M.J. Wagner, Lasers Surg. Med. **12**, 401-409 (1992).